Title
R PARITY BREAKING IN SUPERSYMMETRIC THEORIES

Author
Dawson, S.

Publication Date
1985-04-01

Lawrence Berkeley Laboratory
UNIVERSITY OF CALIFORNIA

Physics Division

Submitted for publication

R PARITY BREAKING IN SUPERSYMMETRIC THEORIES

S. Dawson

April 1985

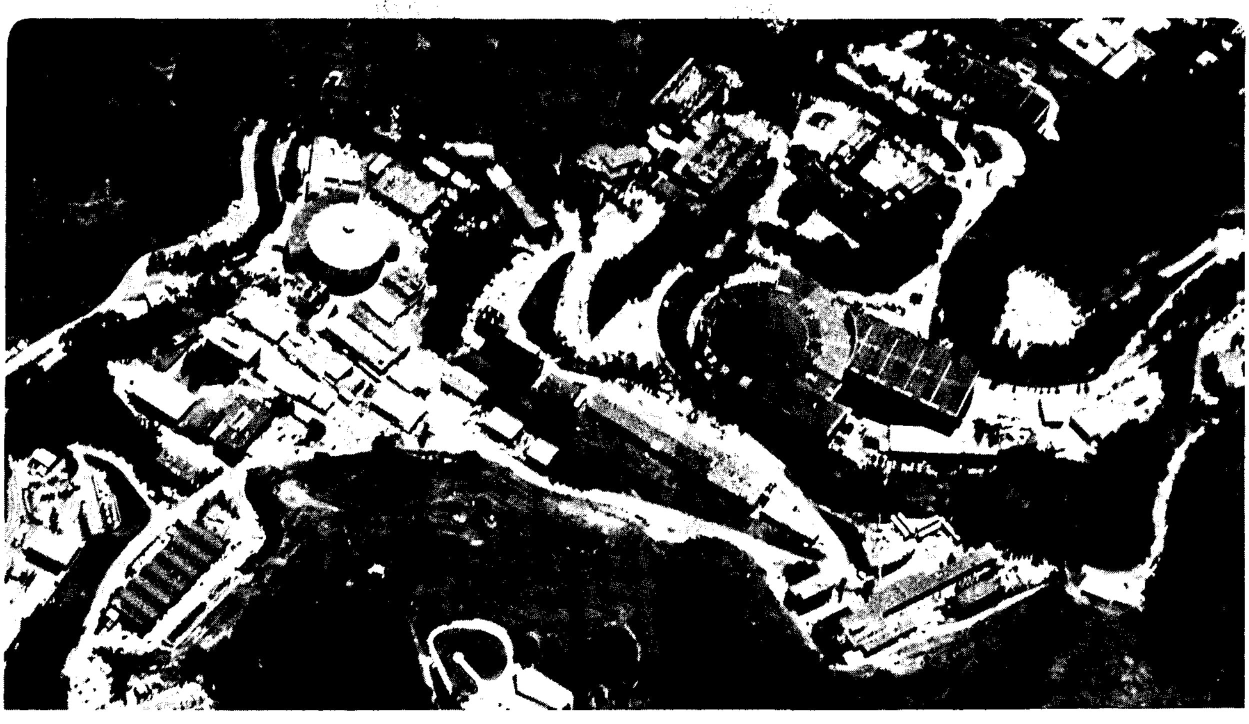

Prepared for the U.S. Department of Energy under Contract DE-AC03-76SF00098

LBL-19460

April, 1985

R PARITY BREAKING IN SUPERSYMMETRIC THEORIES[1]

Sally Dawson

Lawrence Berkeley Laboratory

University of California

Berkeley, California 94720

ABSTRACT

We examine the consequences of R parity breaking in low energy supersymmetric models. This breaking can occur through explicit soft terms in the Lagrangian or through vacuum expectation values of scalar neutrinos. We discuss the new phenomenology expected in this class of models and compare it with the predictions of the R conserving supersymmetric theories.

[1] This work was supported by the Director, Office of Energy Research, Office of High Energy and Nuclear Physics, Division of High Energy Physics of the US Department of Energy under contract DE-AC03-76SF00098.

1 Introduction

The predictions of supersymmetric (SUSY) theories have come under detailed scrutiny in recent months [1]. However, most of the studies have been done assuming an effective low energy SUSY theory in which baryon and lepton number are absolutely conserved [2,3]. This requirement is not dictated by the supersymmetry, but must be imposed by hand. In this paper, we examine the phenomenological consequences of relaxing this assumption. The effects are small, but potentially measurable in e^+e^- and hadron colliders.

Supersymmetric theories have an additively conserved R quantum number which can be defined such that left chiral superfields have R=2/3, vector superfields have R=0, and the anti-commuting θ ($\overline{\theta}$) variable has R=1 (R=-1) [4]. Majorana mass terms for the gauginos certainly break this symmetry since the gauginos have R=1. In addition, the vacuum expectation values of the Higgs bosons which break the SU(2) x U(1) symmetry also break the R symmetry. However, in most supersymmetric models there remains a conserved multiplicative quantum number which we call $\tilde{R}$ parity. Frequently, $\tilde{R}$ parity is a linear combination of R parity and discrete symmetries of the model. The $\tilde{R}$ quantum number is +1 for all of the known fields and -1 for their supersymmetric partners. The $\tilde{R}$ parity of a particle can be written as,

$$\tilde{R} = (-1)^{2S+L+3B} , \qquad (1)$$

where B is the baryon number of the particle, L is the lepton number, and S is the spin. Hence a theory which conserves $\tilde{R}$ parity also conserves baryon and lepton number.

In supersymmetric theories, it is posssible to construct models in which $\tilde{R}$ parity (and hence baryon and lepton number) is violated at an experimentally acceptable level. $\tilde{R}$ parity may be violated explicitely by adding lepton or baryon number violating terms to the Lagrangian or spontaneously by vacuum expectation values (VEVs) of the scalar neutrinos. We will explore both possibilities.

Lepton number violation in SUSY theories has been considered by Hall and Suzuki [5] and by Lee [6]. The allowed values of scalar neutrino VEVs are restricted by the experimental limits on neutrino masses, while the magnitude of explicit lepton number violating terms are constrained by the limits on certain rare processes: $\pi \rightarrow$ e ν, $\mu \rightarrow$ e γ and $\mu \rightarrow$ 3e, for example. Baryon number violating terms are of course restricted by the limits on proton decay.

If $\tilde{R}$ parity breaking terms are allowed in the Lagrangian then the supersymmetric partners of the ordinary particles need not be pair produced and many new reactions will be allowed such as $p\overline{p} \rightarrow \tau\tilde{\gamma}$ or $p\overline{p} \rightarrow \tau\tilde{q}$. Many of the most interesting new processes will contain single leptons in the final state and the experimental signals will be strikingly different from those of the standard SUSY model. This new phenomenology has been explored by Ellis et al.[7]. In addition, if the scalar neutrinos have VEVs, then there will be mass mixing between the charged leptons and the fermionic partners of the W bosons (winos) and the fermionic partners of the charged Higgs bosons (Higgsinos). There will also be mixing in the neutral sector between the

neutrinos and the photino,zino, and neutral Higgsinos. Mass mixing caused by $\tilde{R}$ parity breaking has been studied in Refs. [6] and [7].

This paper is organized as follows: In Section 2, we discuss the model which we consider in the remainder of this paper. It is an effective low energy SU(3) x SU(2) x U(1) supersymmetric model which contains terms which explicitely violate lepton and baryon number. We examine the scalar potential and show that in general the scalar neutrinos will get VEVs and spontaneously break $\tilde{R}$ [8]. Our analysis of the scalar potential is similar to that of Ross and Valle [9] who showed that in the hidden sector supergravity models [10] the τ sneutrino naturally gets a VEV. The limits on the magnitude of the $\tilde{R}$ violating terms are reviewed in Section 3. Many of these limits have been obtained by Hall and Suzuki [5] and by Lee [6], but we include them here for completeness. Our most important results are contained in Section 4 where we consider the new physics predicted by this model. In particular, there will be single production of SUSY particles and new decay chains for the SUSY particles. We end by comparing the predictions of our model with those of the standard $\tilde{R}$ conserving SUSY model.

2 A SUSY Model with $\tilde{R}$ Parity Breaking

We consider an effective low energy supersymmetric Lagrangian. The model has three generations of left chiral matter superfields,

$$\begin{array}{ll} Q_a(3,2,1/6) & L_a(1,2,-1/2) \\ \overline{U}_a(\overline{3},1,-2/3) & \overline{E}_a(1,1,1) \\ \overline{D}_a(\overline{3},1,1/3), & \end{array} \qquad (2)$$

where the SU(3) x SU(2) x U(1) quantum numbers are shown in parenthesis and a is a generation index. The model also has two Higgs superfields,

$$H(1,2,1/2) \quad H'(1,2,-1/2) \ , \tag{3}$$

and three vector superfields, G(8,1,1),W(1,3,1) and B(1,1,1) in the adjoint representations of the gauge groups. If we assume that the supersymmetry is softly broken then the most general SU(3) x SU(2) x U(1) invariant Lagrangian with the fields listed above which conserves baryon and lepton number is,

$$\mathcal{L}_{lc} = \mathcal{L}_{Kinetic} + \mathcal{L}_{Soft} + \mathcal{L}_{Yukawa}, \tag{4}$$

where,

$$\begin{aligned} \mathcal{L}_{Soft} \ &= \{\mu_1 \tilde{\psi}_{W^+}\tilde{\psi}_{W^-} - \mu_2 \tilde{\psi}_{H'^-}\tilde{\psi}_{H^+} + igv_1 \tilde{\psi}_{W^-}\tilde{\psi}_{H^+} \\ &+ igv_2 \tilde{\psi}_{W^+}\tilde{\psi}_{H'^-} + \tfrac{1}{2}\mathcal{M}_1 \tilde{\psi}_A \tilde{\psi}_A + \mathcal{M}_2 \tilde{\psi}_A \tilde{\psi}_Z \\ &+ \tfrac{1}{2}\mathcal{M}_3 \tilde{\psi}_Z \tilde{\psi}_Z - iM_Z \tilde{\psi}_Z \tilde{\psi}_h \ - \mu_4^2(\phi_{H'^-}\phi_{H^+} - \phi_{H'^o}\phi_{H^o}) \\ &- \tfrac{1}{2}\Sigma_i M_i^2 \mid \phi_i \mid^2 - \mu_2[\tfrac{1}{2}\sin 2\theta(\tilde{\psi}_h \tilde{\psi}_h - \tilde{\psi}_{h'}\tilde{\psi}_{h'}) \\ &+ \cos 2\theta \tilde{\psi}_h \tilde{\psi}_{h'}] + \tfrac{1}{2} m_{\tilde{g}} \tilde{\psi}_G \tilde{\psi}_G\} + \text{h.c.} \\ &+ \text{terms cubic in the scalar fields,} \end{aligned} \tag{5}$$

and $\tilde{\psi}_A$, $\tilde{\psi}_G$, $\tilde{\psi}_W$, and $\tilde{\psi}_Z$ are the two component Majorana gauginos associated with the photon,gluon and W and Z gauge bosons, $\tilde{\psi}_H$ and $\tilde{\psi}_{H'}$ are the fermionic partners of the Higgs bosons , $v_1 = \langle \phi_{H^o} \rangle$ and $v_2 = \langle \phi_{H'^o} \rangle$. The soft masses μ_i and M_i are arbitrary and all of the spinors ψ_i are written in two component notation. Our notation is such that the superpartners of the ordinary particles are denoted by tildes. The term

$\Sigma M_i^2 \mid \phi_i \mid^2$ sums over all scalar fields in the theory and,

$$\begin{aligned} \mathcal{M}_1 \ &= \sin^2 \theta_W \mu_1 + \cos^2 \theta_W \mu_3 \\ \mathcal{M}_2 \ &= e(\mu_1 - \mu_3) \\ \mathcal{M}_3 \ &= \cos^2 \theta_W \mu_1 + \sin^2 \theta_W \mu_3 \\ \tilde{\psi}_h \ &= \tilde{\psi}_{H^o} \cos\theta + \tilde{\psi}_{H'^o} \sin\theta \\ \tilde{\psi}_{h'} \ &= \tilde{\psi}_{H'^o} \cos\theta - \tilde{\psi}_{H^o} \sin\theta \ , \end{aligned} \tag{6}$$

where θ_W is the Weinberg angle and $\tan\theta = -v_2/v_1$. $\mathcal{L}_{Yukawa}$ can be written in terms of the superfields as,

$$\begin{aligned} \mathcal{L}_{Yukawa} = \ &\int d^2\theta [g_{U_{ab}} \overline{U}_a H Q_b + g_{D_{ab}} \overline{D}_a H' Q_b + g_{E_{ab}} \overline{E}_a H' L_b] \\ &+ \text{h.c.} \end{aligned} \tag{7}$$

Two types of explicit $\tilde{R}$ violating interactions can be included in the Lagrangian,

$$\mathcal{L}_{lv} = \mathcal{L}_1 + \mathcal{L}_2 \ . \tag{8}$$

$\mathcal{L}_1$ consists of the dimension two soft operators coupling the scalar components of the Higgs doublet superfields, ϕ_H and $\phi_{H'}$,to the scalar members of the lepton doublet superfield, $\tilde{\phi}_L$,

$$\mathcal{L}_1 = -\tilde{m}_{1a}^2 \phi_H \tilde{\phi}_{L_a} - \tilde{m}_{2a}^2 \phi_{H'}^\dagger \tilde{\phi}_{L_a} + \ \text{h.c.} \tag{9}$$

(Note that an $H'^\dagger L$ term coupling the superfields is not invariant under the supersymmetry. However the $\phi_{H'}^\dagger \phi_{L_a}$ term is included in $\mathcal{L}_1$ for generality.)

In addition, we can include the lepton and baryon number violating terms resulting from the $\theta\theta$ term of $Q\overline{D}$L, $L\overline{E}$L, and $\overline{UDD}$. Such terms could result from a supersymmetric theory coupled to N=1 supergravity [5]. These terms are,

$$\begin{aligned} \mathcal{L}_2 = \ &-C_a(\psi_{u_{La}}\psi_{\overline{d}_{La}}\tilde{\phi}_{e_{La}} + \psi_{d_{La}}\psi_{\overline{d}_{La}}\tilde{\phi}_{\nu_{La}} + ...) - D_a(\psi_{e_{La}}\psi_{\overline{e}_{La}}\tilde{\phi}_{\nu_{La}} \\ &+ ...) - E_a(\psi_{\overline{u}_{La}}\psi_{\overline{d}_{La}}\tilde{\phi}_{\overline{d}_{La}} + ...) + \ \text{h.c.} \ , \end{aligned} \tag{10}$$

where the . . . indicate SUSY permutations of the fields and the coefficients C_a, D_a, and E_a are arbitrary. ($\psi_{u_{La}}$ is the left-handed charge 2/3 quark of generation a and $\tilde{\phi}_{u_{La}}$ is the associated scalar, etc.) For simplicity, we have assumed that the $\tilde{R}$ violating terms of Eq. (10) are diagonal in generation space [11].

The Lagrangians of Eqs.(9) and (10) can easily be forbidden by imposing discrete symmetries. For example, $\tilde{\phi}_L \to -\tilde{\phi}_L$ forbids $\mathcal{L}_1$ and Q → -Q, $\overline{U} \to -\overline{U}$, and $\overline{E} \to -\overline{E}$ forbids $\mathcal{L}_2$. There are many possibilities for such discrete symmetries.

2.1 Masses and Mixing

Lepton number violation also arises from the VEVs of the scalar neutrinos. These VEVs introduce mass mixing among the charged and neutral fermions. The charged mass eigenstates are $\chi^+ = U^\dagger\Psi^+$ and $\chi^- = V^\dagger\Psi^-$ where,

$$\Psi^+ = \begin{pmatrix} -i\tilde{\psi}_{W^+} \\ \tilde{\psi}_{H^+} \\ \psi_{L_a^+} \end{pmatrix} \tag{11}$$

and,

$$\Psi^- = \begin{pmatrix} -i\tilde{\psi}_{W^-} \\ \tilde{\psi}_{H'^-} \\ \psi_{L_a^-} \end{pmatrix}. \tag{12}$$

U and V are 5 x 5 unitary matrices which are determined by diagonalizing the mass matrix,

$$M^+ = \begin{pmatrix} \mu_1 & gv_1 & 0 \\ gv_2 & \mu_2 & \lambda_c\tilde{v}_a \\ g\tilde{v}_a & 0 & \lambda_a v_2 \end{pmatrix}, \tag{13}$$

where $\tilde{v}_a$ are the VEVs of the scalar neutrinos, λ_a is fixed by the requirement that the leptons have their physical masses and,

$$\mathcal{L}_M = -\Psi^{-T}M^+\Psi^+ + \text{h.c.} \tag{14}$$

In general, this matrix must be diagonalized numerically. As an example, we consider the case of unbroken supersymmetry where only the $\tilde{\nu}_\tau$ gets a VEV. In this case, μ_1=μ_2=0 and gv_1=gv_2=M_W. The mass terms in the Lagrangian are,

$$\mathcal{L}_M = -\tilde{\psi}^{-T}\tilde{M}^+\tilde{\psi}^+ - m_e\psi_e\psi_e - m_\mu\psi_\mu\psi_\mu + \text{ h.c. }, \tag{15}$$

where,

$$\tilde{M}^+ = \begin{pmatrix} \lambda_\tau M_W/g & g\tilde{v}_\tau & 0 \\ \lambda_\tau\tilde{v}_\tau & M_W & 0 \\ 0 & 0 & M_W \end{pmatrix} \tag{16}$$

and

$$\tilde{\psi}^+ = \begin{pmatrix} \psi_{\tau^+} \\ -i\tilde{\psi}_{W^+} \\ \tilde{\psi}_{H^+} \end{pmatrix} \tag{17}$$

$$\tilde{\psi}^- = \begin{pmatrix} \psi_{\tau^-} \\ \tilde{\psi}_{H'^-} \\ -i\tilde{\psi}_{W^-} \end{pmatrix}. \tag{18}$$

The eigenstates and eigenvalues are easily found in this example,

$$\begin{aligned} \chi_1^+ &= \tilde{\psi}_{H^+} \\ \chi_1^- &= -i\tilde{\psi}_{W^-} \end{aligned} \tag{19}$$

with mass M_W,

$$\begin{aligned} \chi_2^+ &= -i\tilde{\psi}_{W^+} + m_\tau\epsilon/M_W\psi_{\tau^+} \\ \chi_2^- &= m_\tau\epsilon/M_W\psi_{\tau^-} + \tilde{\psi}_{H'^-} \end{aligned} \tag{20}$$

with mass $M_W + m_\tau \epsilon^2$ and

$$\begin{aligned} \chi_3^+ &= \psi_{\tau^+} + i\epsilon m_\tau / M_W \tilde{\psi}_{W^+} \\ \chi_3^- &= \psi_{\tau^-} - m_\tau \epsilon / M_W \tilde{\psi}_{H'^-} \end{aligned} \tag{21}$$

with mass m_τ , where we have worked to leading order in ϵ and m_τ/M_W and,

$$\epsilon \equiv \frac{\tilde{v}_\tau}{v_1} \, . \tag{22}$$

In this example all effects of the $\tilde{R}$ violation are suppressed by powers of ϵ. In general, mixing between the charged leptons and winos and Higgsinos is suppressed by powers of $\tilde{v}_a/v_1$ or $\tilde{v}_a/v_2$ as is obvious from Eq.(13).

The mixing in the neutral sector is similar to that in the charged sector. The neutral fermion mass matrix is,

$$M^o = \begin{pmatrix} \mathcal{M}_1 & \mathcal{M}_2 & 0 & 0 & 0 \\ \mathcal{M}_2 & \mathcal{M}_3 & -M_Z & 0 & g\tilde{v}_a/(\sqrt{2}\cos\theta_W) \\ 0 & -M_Z & \mu_2 \sin 2\theta & \mu_2 \cos 2\theta & 0 \\ 0 & 0 & \mu_2 \cos 2\theta & -\mu_2 \sin 2\theta & 0 \\ 0 & g\tilde{v}_a/(\sqrt{2}\cos\theta_W) & 0 & 0 & 0 \end{pmatrix} \tag{23}$$

where,

$$\mathcal{L} = -\frac{1}{2}\Psi^{oT} M^o \Psi^o + \text{ h.c.} \tag{24}$$

and

$$\Psi^o = \begin{pmatrix} -i\tilde{\psi}_A \\ -i\tilde{\psi}_Z \\ \tilde{\psi}_h \\ \tilde{\psi}_{h'} \\ \psi_{\nu_a} \end{pmatrix} . \tag{25}$$

Only one linear combination of the neutrinos, ν_M, participates in the mass mixing of Eq.(23) and gets a Majorana mass

at tree level,

$$\nu_M = \sum_a \tilde{v}_a \nu_a \Big/ \sqrt{\sum_a \tilde{v}_a^2} \, . \tag{26}$$

The two orthogonal combinations of neutrinos remain massless at tree level. Limits on sneutrino VEVs from neutrino masses will be discussed in detail in Section 3.

In the example of unbroken supersymmetry discussed above ($\mu_1 = \mu_2 = \mu_3 = 0$ and $gv_1 = gv_2 = M_W$) where the only nonzero sneutrino VEV is $\tilde{v}_\tau$, there are three zero mass eigenvalues,

$$\begin{aligned} \chi_1^o &= -i\tilde{\psi}_A \\ \chi_2^o &= \tilde{\psi}_{h'} \\ \chi_3^o &= \epsilon/\sqrt{2}\tilde{\psi}_h + \psi_\nu + \mathcal{O}(\epsilon^2) \, . \end{aligned} \tag{27}$$

χ_1^o and χ_2^o may be combined to form a Dirac photino. In addition, there are two massive eigenvectors,

$$\begin{aligned} \chi_4^o &= i/\sqrt{2}\tilde{\psi}_Z - 1/\sqrt{2}\tilde{\psi}_h + \epsilon/2\psi_\nu + \mathcal{O}(\epsilon^2) \\ \chi_5^o &= i/\sqrt{2}\tilde{\psi}_Z + 1/\sqrt{2}\tilde{\psi}_h - \epsilon/2\psi_\nu + \mathcal{O}(\epsilon^2) \end{aligned} \tag{28}$$

with masses $\pm M_Z(1+\epsilon^2/4) + \mathcal{O}(\epsilon^3)$. Again, all mixing effects are suppressed by powers of the sneutrino VEVs.

There is also mixing in the scalar sector between the Higgs bosons and the scalar partners of the leptons. We will consider only the mixing in the imaginary neutral scalar sector. One linear combination of Im ϕ_H and Im $\phi_{H'}$ becomes the longitudinal component of the Z gauge boson and for a one generation model there are two physical scalars, $\tilde{\phi}_1$ and $\tilde{\phi}_2$. $\tilde{\phi}_1$ couples to the lepton current and is a would be Majoron [8]. However the coupling of $\tilde{\phi}_1$ to the fermions is proportional to gM_f/M_W and hence there is no $\tilde{\phi}_1 \nu \overline{\nu}$ coupling and so no problem with Majoron emission in μ or K decay. The only limits on $\tilde{\phi}_1$ come from energy losses in red giants via Majoron emission [12]. However, if the Majoron is heavier than the temperature of the red giant (10 Mev $\sim 10^8\,{}^\circ$ K) then there are no limits on the Majoron mass. From Eq. (5), we see that $\tilde{\phi}_1$ will get a mass on the order of the soft scalar masses associated with $\tilde{\phi}_L, \phi_H$, or $\phi_{H'}$. As long as these masses are greater than 10 MeV, models of the type we are considering will not have problems with Majorons.

2.2 Scalar Potential

We turn now to a discussion of the scalar potential. We consider a toy model with only one generation of fermions in which the scalar potential is given by ,

$$\begin{aligned} V = \; & [\tilde{m}_1{}^2\phi_H\tilde{\phi}_L + \tilde{m}_2^2\phi^\dagger_{H'}\tilde{\phi}_L + \mu_4^2\phi_H\phi_{H'} - \tilde{\phi}_{\overline{E}}(m_{E'}\phi_{H'} + m_E\phi^\dagger_H)\tilde{\phi}_L \\ & -\tilde{\phi}_{\overline{D}}(m_{D'}\phi_{H'} + m_D\phi^\dagger_H)\tilde{\phi}_Q - \tilde{\phi}_{\overline{U}}(m_U\phi_H + m_{U'}\phi^\dagger_{H'})\tilde{\phi}_Q \\ & + \text{h.c.}] + M_H^2 \mid \phi_H \mid^2 + M_{H'}^2 \mid \phi_{H'} \mid^2 + M_L^2 \mid \tilde{\phi}_L \mid^2 \\ & + M_E^2 \mid \tilde{\phi}_{\overline{E}} \mid^2 + M_Q^2 \mid \tilde{\phi}_Q \mid^2 + M_D^2 \mid \tilde{\phi}_{\overline{D}} \mid^2 + M_U^2 \mid \tilde{\phi}_{\overline{U}} \mid^2 \\ & + \tfrac{1}{2}g'^2[\tfrac{1}{2} \mid \phi_H \mid^2 - \tfrac{1}{2} \mid \phi_{H'} \mid^2 - \tfrac{1}{2} \mid \tilde{\phi}_L \mid^2 + \mid \tilde{\phi}_{\overline{E}} \mid^2 + \tfrac{1}{6} \mid \tilde{\phi}_Q \mid^2 \\ & + \tfrac{1}{3} \mid \tilde{\phi}_{\overline{D}} \mid^2 - \tfrac{2}{3} \mid \tilde{\phi}_{\overline{U}} \mid^2]^2 + \tfrac{1}{8}g^2[\phi^\dagger_H\sigma\phi_H + \phi^\dagger_{H'}\sigma\phi_{H'} \\ & + \tilde{\phi}^\dagger_L\sigma\tilde{\phi}_L + \tilde{\phi}^\dagger_Q\sigma\tilde{\phi}_Q]^2 + \mid g_E\tilde{\phi}_{\overline{E}}\tilde{\phi}_L + g_D\tilde{\phi}_{\overline{D}}\tilde{\phi}_Q \mid^2 + \mid g_E\phi_{H'}\tilde{\phi}_L \mid^2 \\ & + \mid g_E\tilde{\phi}_{\overline{E}}\phi_{H'} \mid^2 + \mid g_U\tilde{\phi}_{\overline{U}}\tilde{\phi}_Q \mid^2 + \mid g_D\tilde{\phi}_{\overline{D}}\phi_{H'} + g_U\tilde{\phi}_{\overline{U}}\phi_H \mid^2 \\ & + \mid g_D\phi_{H'}\tilde{\phi}_Q \mid^2 + \mid g_U\phi_H\tilde{\phi}_Q \mid^2 + \text{SU(3) D term} , \end{aligned} \tag{29}$$

where g' and g are the U(1) and SU(2) gauge coupling constants, respectively. In general, all of the neutral scalars can receive VEVs and minimizing the potential yields the restrictions on the allowed VEVs,

$$\begin{aligned} -\tilde{m}_2^2\tilde{v}_1/v_2 + \mu_4^2 v_1/v_2 = \; & M_{H'}^2 - \tfrac{1}{4}(g'^2 + g^2)(v_1^2 - v_2^2 - \tilde{v}_1^2) + \; g_E^2\tilde{v}_1^2 \\ \tilde{m}_1^2\tilde{v}_1/v_1 + \mu_4^2 v_2/v_1 = \; & M_H^2 + \tfrac{1}{4}(g'^2 + g^2)(v_1^2 - v_2^2 - \tilde{v}_1^2) \\ \tilde{m}_1^2 v_1/\tilde{v}_1 - \tilde{m}_2^2 v_2/\tilde{v}_1 = \; & M_L^2 - \tfrac{1}{4}(g'^2 + g^2)(v_1^2 - v_2^2 - \tilde{v}_1^2) + \; g_E^2 v_2^2 \,. \end{aligned} \tag{30}$$

The allowed VEVs can easily be found by neglecting the small Yukawa coupling g_E and by setting $v_1/v_2 = -\cot\theta$ and $\tilde{v}_1/v_2 = \tan\gamma$. In the limit in which the soft mass terms are equal,

$$\begin{aligned} \tilde{m}_1 = \tilde{m}_2 \equiv \tilde{m} \\ M_L = M_H = M_{H'} \equiv \tilde{M} \,, \end{aligned} \tag{31}$$

the allowed VEVs are given by the equations,

$$\begin{aligned} 0 = \; & \tan^3\gamma[-\tilde{m}^6 + \mu_4^2\tilde{m}^2(2\tilde{M}^2 - \mu_4^2)] + \tan^2\gamma[3\mu_4^2\tilde{m}^4 - \mu_4^6 \\ & -2\tilde{M}^2\tilde{m}^4] + \tan\gamma(2\tilde{m}^2\mu_4^2)(\mu_4^2 - \tilde{M}^2) \; - 2\tilde{m}^4(\mu_4^2 - \tilde{M}^2) \\ \cot\theta = \; & \tilde{m}^2(\tan^2\gamma - 1)/(\tilde{m}^2 - \mu_4^2\tan\gamma) \\ v_2 = \; & \sqrt{2}\; M_W/(g\sqrt{\tan^2\gamma + \csc^2\theta}) \,. \end{aligned} \tag{32}$$

The results for $\tan\gamma$ are shown in Figure 1 for different values of μ_4,$\tilde{m}$, and $\tilde{M}$. Note that even for quite small values of $\tilde{m}$, $\tilde{v}_1$ can be of the same order of magnitude as v_1 . From Eq. (32) it is obvious, however, that for $\tilde{m} \to 0$, the sneutrino VEV, $\tilde{v}_1$, also vanishes.

3 Limits on $\tilde{R}$ Violation

3.1 Neutrino Masses

The most severe limitations on $\tilde{R}$ violation come from limits on neutrino masses. We will assume that the neutrino which gets a Majorana mass, ν_M, is ν_τ. In this case we must have $m_{\nu_M} \leq 143$ MeV [13]. Assuming the parameters μ_i of Eq. (5) are equal and much larger than M_Z, the mass matrix of Eq.(23) gives the restrictions,

$$\sqrt{\sum_a \tilde{v}_a^2} \leq \begin{cases} 12 \text{ GeV} & \text{if } \mu_i = 250 \text{ GeV} \\ 24 \text{ GeV} & \text{if } \mu_i = 1 \text{ TeV} \end{cases} \,. \tag{33}$$

If ν_M is ν_e or ν_μ then the restrictions on the sneutrino VEVs are considerably stricter. For example, if ν_M is ν_e, then requiring $m_{\nu_e} \leq 6$ eV (the limit from neutrino-less double beta decay) we have,

$$\sqrt{\sum_a \tilde{v}_a^2} \leq \begin{cases} 2 \text{ MeV} & \text{if } \mu_i = 250 \text{ GeV} \\ 5 \text{ MeV} & \text{if } \mu_i = 1 \text{ TeV} \end{cases} . \tag{34}$$

In addition, the sneutrino VEVs and the explicit lepton number violating terms of Eq.(10) lead to one loop masses for the ν_e, ν_μ, and ν_τ neutrinos. We will calculate one of these contributions as an example and require that the contribution of each diagram satisfy the limits on neutrino masses. For a discussion of the limits on neutrino masses in a theory with $\tilde{R}$ viclation and SUSY coupled to N=1 supergravity see Ref. [5]. The diagram of Figure 2 contributes a factor to the neutrino mass matrix,

$$\begin{aligned} &\Sigma_a \mathcal{U}_{ia}\mathcal{U}_{ja} g^2 \tilde{v}_a m_{\tilde{w}} m_{l_a} D_a/[16\pi^2(m_{\tilde{w}}^2 - m_{l_a}^2)]\{m_{\tilde{w}}^2/(m_{\tilde{l}_a}^2 - m_{\tilde{w}}^2) \\ &\quad \text{x } \ln(m_{\tilde{l}_a}^2/m_{\tilde{w}}^2) + m_{l_a}^2/(m_{\tilde{l}_a}^2 - m_{l_a}^2)\ln(m_{l_a}^2/m_{\tilde{l}}^2)\}\nu_i^!\nu_j^! \,, \end{aligned} \tag{35}$$

where a is again a generation index , m_{l_a} is the charged lepton mass, $m_{\tilde{w}}$ is the wino mass, $\nu_i^!$ is the physical electron, muon, or tau neutrino, and $\mathcal{U}$ is the unitary matrix which diagonalizes the neutral fermion mass matrix. In the limit $m_{\tilde{w}} = m_{\tilde{l}_a} \equiv \tilde{M} \gg m_{l_a}$, this reduces to,

$$\sum_a \mathcal{U}_{ia}\mathcal{U}_{ja} g^2 \tilde{v}_a (m_{l_a}/\tilde{M}) D_a/(16\pi^2)\nu_i^!\nu_j^! \,. \tag{36}$$

Requiring $m_{\nu_e} \leq 6$ eV, $m_{\nu_\mu} \leq 520$ KeV, $m_{\nu_\tau} \leq 143$ MeV and taking $\mathcal{U}_{ai} = \delta_{ai}$, Eq. (36) gives the restrictions,

$$\begin{aligned} &D_e \lesssim 10^2(\tilde{M}/250 \text{ GeV})(10 \text{ MeV}/\tilde{v}_e) \\ &D_\mu \lesssim 5 \text{ x } 10^4(\tilde{M}/250 \text{ GeV})(10 \text{ MeV}/\tilde{v}_\mu) \\ &D_\tau \lesssim 10^6(\tilde{M}/250 \text{ GeV})(10 \text{ MeV}/\tilde{v}_\tau) \,. \end{aligned} \tag{37}$$

Hence quite large values of the coupling D_a are allowed.

3.2 Rare Processes

The limits on explicit lepton number violating interactions from rare processes have been found in Refs. [5] and [6] and we summarize them here in our notation. We have taken all of the soft masses $(M_L, M_E, M_Q, M_D, M_U)$ equal to $\tilde{M}$ and neglected the photino mass in these limits.

1. $\pi \to e\tilde{\gamma}$ gives,
   $C_1 V_{ee}^\dagger \lesssim 2 \text{ x } 10^{-3}(\tilde{M}/100 \text{ GeV})^2$,

2. $\mu \to$ 3 e gives,
   $C_1^2 V_{\mu e}^\dagger V_{ee}^\dagger + C_2^2 V_{\mu\mu}^\dagger V_{e\mu}^\dagger + C_3^2 V_{\mu\tau}^\dagger V_{e\tau}^\dagger \lesssim 5 \text{ x } 10^{-5}(\tilde{M}/100 \text{ GeV})^2$,
   $D_1^2 V_{\mu e}^\dagger V_{ee}^\dagger + D_2^2 V_{\mu\mu}^\dagger V_{e\mu}^\dagger + D_3^2 V_{\mu\tau}^\dagger V_{e\tau}^\dagger \lesssim 5 \text{ x } 10^{-5}(\tilde{M}/100 \text{ GeV})^2$,

3. $\mu \to e\gamma$ gives,
   $D_1 V_{\mu e}^\dagger V_{ee}^\dagger(\tilde{v}_e/10 \text{ MeV}) + D_2 V_{e\mu}^\dagger\ V_{\mu\mu}^\dagger(\tilde{v}_\mu/10 \text{ MeV})$
   $\lesssim 10^{-5}(\tilde{M}/100 \text{ GeV})^2$.

(38)

Because of our assumption that the explicit lepton number violating terms of Eq. (10) are diagonal in generation space, there is no contribution to processes such as K $\to e\tilde{\gamma}$ or $K_L K_S$ mixing.

The surprise is that $C_i \sim 10^{-3}$ is completely consistent with all experimental limits on lepton number violating processes even for $\tilde{M}$ as small as 100 GeV. The limits on D_i from $\mu \to e\gamma$ are slightly stronger than the limits on C_i if the mixing angle, $V_{e\mu}$, is near 1. However, $D_i \sim 10^{-3}$ is allowed for $\tilde{M} \sim 1$ TeV and $\tilde{v}_i \sim 10$ MeV for any value of the mixing angle.

In addition, requiring the proton lifetime to be larger than 10^{32} years imposes the restriction that $E_1 \lesssim 10^{-39}(10^{-3}/C_1)(\tilde{M}/100 \text{ GeV})^4$. Since E_1 is forced to be so small, we will not consider further the effects of such a term.

4 Phenomenology of $\tilde{R}$ Violating Theories

In this section, we describe the new phenomenology predicted by the $\tilde{R}$ violating SUSY theories described in Section 2. These effects fall into three categories: (i) Single production of SUSY particles, (ii) New decay modes of the photino and sneutrino, and (iii) New experimental signatures as the result of the different decay modes. We will examine each of the consequences in turn.

4.1 Single production of SUSY Particles

In the model of Section 2, SUSY particles can be produced singly either due to mixing effects or due to the explicit $\tilde{R}$ violating terms in the Lagrangian. A wide range of reactions such as $p\overline{p} \to \nu\tilde{W}$, $\tilde{q}$ e, $\tilde{Z}$ e, etc. are possible in theories with broken $\tilde{R}$. However, the cross sections tend to be miniscule unless the SUSY particles are light ($\sim$ several GeV). As an example, we consider $l_a\tilde{\gamma}$ and $l_a\tilde{g}$ production in detail , (l_a is e, μ, or τ).

The reaction $p\overline{p} \to l_a\tilde{\gamma}$ procedes by t- and u-channel squark exchange and by s-channel W boson exchange. Neglecting the lepton mass and assuming all of the squarks are degenerate, the cross section can be written as,

$$\begin{aligned}\sigma(q_i\overline{q_j} \to l_a\tilde{\gamma}) = \ & (\pi/s^2)\left\{A_s S/(3(s-M_W^2)^2)(2s^2 - sm_{\tilde{\gamma}}^2 - m_{\tilde{\gamma}}^4)\right. \\ & + \left[A_t\left(S + (m_{\tilde{q}}^2+\Delta)\Lambda + S\Delta/(s+\Delta)\right)\right. \\ & + A_{st}/(s-M_W^2)\left(S(m_{\tilde{q}}^2 - (s+m_{\tilde{\gamma}}^2)/2) + \Delta m_{\tilde{q}}^2\Lambda\right) \\ & \left.\left. +(t\to u)\ \right]\right\}\end{aligned} \tag{39}$$

where,

$$\begin{aligned}\Delta &= m_{\tilde{q}}^2 - m_{\tilde{\gamma}}^2 \\ \Lambda &= ln\left[(s+\Delta+m_{\tilde{q}}^2 - S)/(s+\Delta+m_{\tilde{q}}^2+S)\right] \\ S &= s - m_{\tilde{\gamma}}^2\ ,\end{aligned} \tag{40}$$

and the coefficients A_i are,

$$\begin{aligned}A_t &= (\alpha^2 e_{q_j}^2)/(6\sin^2\theta_W)\mid V_{l_a\tilde{w}}^\dagger - iC_a/g\mid^2 \\ A_u &= (\alpha^2 e_{q_i}^2)/(6\sin^2\theta_W)\mid U_{\tilde{w}l_a} - iC_a/g\mid^2 \\ A_{su} &= (\alpha^2 e_{q_i})/(3\sin^2\theta_W)\mid U_{\tilde{w}l_a} - iC_a/g\mid^2 \\ A_{st} &= -(\alpha^2 e_{q_j})/(3\sin^2\theta_W)\mid V_{l_a\tilde{w}}^\dagger - iC_a/g\mid^2 \\ A_s &= (\alpha^2)/(12\sin^2\theta_W)(\mid U_{\tilde{w}l_a} - iC_a/g\mid^2 + \mid V_{l_a\tilde{w}}^\dagger - iC_a/g\mid^2)\,.\end{aligned} \tag{41}$$

(We have neglected the generalized KM mixing between the quarks and the squarks in Eq. (41)). C_a is the coefficient of the $U_a\overline{D}_aL_a$ term in the Lagrangian of Eq. (10) and V and U are the matrices which diagonalize the charged fermion mass matrix (defined above Eq. (11)).

The reaction $p\overline{p} \to l_a\tilde{g}$ occurs through t- and u- channel squark exchange. The cross section is given by Eqs. (39) and (40) with the replacement $m_{\tilde{\gamma}} \to m_{\tilde{g}}$. The coefficients A_i are,

$$\begin{aligned}A_s &= A_{st} = A_{su} = 0 \\ A_t &= (2\alpha_s\alpha)/(9\sin^2\theta_W)\mid V_{l_a\tilde{w}}^\dagger - iC_a/g\mid^2 \\ A_u &= (2\alpha_s\alpha)/(9\sin^2\theta_W)\mid U_{\tilde{w}l_a} - iC_a/g\mid^2\ .\end{aligned} \tag{42}$$

To get an idea of the magnitude of the cross sections, we consider the case where the only violation of $\tilde{R}$ comes from the τ sneutrino VEV and there are no soft mass terms ($\mu_1 = \mu_2 = \mu_3 = 0$) and $v_1 = v_2 \equiv v$. In this case, $V_{\tau\tilde{w}}^\dagger = 0$ and $U_{\tau\tilde{w}}^\dagger = -m_\tau\tilde{v}_3/(M_W v) + O(\tilde{v}_3{}^2/v^2)$.

The numerical results are shown in Figure 3 for $p\overline{p} \to \tilde{g}\tau$ at $\sqrt{s} = 540$ GeV and 2 TeV. (We have taken $\tilde{v}_\tau = 20$ GeV in this example, but the results scale as $\tilde{v}_\tau^2$). If the photino is light, ($m_{\tilde{\gamma}} \sim 1$ GeV), then the cross section for $\tilde{\gamma}\tau$ production will be several orders of magnitude smaller than that for light gluino plus tau production. The cross sections are small since they are suppressed by powers of m_τ^2/M_W^2. However, the experimental signals for $l_a\tilde{g}$ or $l_a\tilde{\gamma}$ production are quite striking. The reaction $p\overline{p} \rightarrow l_a\tilde{g}$ will be signaled by an isolated lepton recoiling against a single jet, while $p\overline{p} \rightarrow l_a\tilde{\gamma}$ will produce a single lepton with no other energetic tracks.

4.2 New Decays

In most SUSY models, the lightest supersymmetric particle is taken to be the photino and it is assumed to be stable. However, in theories with $\tilde{R}$ violation, the photino can decay in several ways,

$$\begin{array}{ll} i) & \tilde{\gamma} \rightarrow \gamma\nu \\ ii) & \tilde{\gamma} \rightarrow q\overline{q}\nu \\ iii) & \tilde{\gamma} \rightarrow u_a\overline{d}_a l_a \\ iv) & \tilde{\gamma} \rightarrow l_a\overline{l}_a\nu \ . \end{array} \tag{43}$$

In addition , the sneutrino can decay to a neutrino - anti neutrino pair.

The decay $\tilde{\gamma} \rightarrow \gamma\nu$ can occur either because of the explicit $\tilde{R}$ violating terms in the Lagrangian or because of the presence of sneutrino VEVs. In the case where the dominant contribution is from the explicit terms in $\mathcal{L}_{lv}$, the diagrams of Figure 4 contribute to the photino decay . The largest contribution is from

Figure 4a and has been calculated in Ref. [5],

$$\Gamma_1(\tilde{\gamma} \rightarrow \gamma\nu + \gamma\overline{\nu}) \sim 9\alpha^2 m_{\tilde{\gamma}}^3/(64\pi^3)[C_a e_{q_a}^2 m_{q_a}/m_{\tilde{q}_a}^2(\ln(m_{q_a}^2/m_{\tilde{q}_a}^2) + \tfrac{3}{2}) + D_a m_{l_a}/m_{\tilde{l}_a}^2(\ln(m_{l_a}^2/m_{\tilde{l}_a}^2) + \tfrac{3}{2})]^2 \ , \tag{44}$$

where m_{q_a} (m_{l_a}) are the quark (lepton) masses, e_{q_a} are the quark charges, and $m_{\tilde{q}_a}$ ($m_{\tilde{l}_a}$) are the squark (slepton) masses. In practice, the largest contribution comes from the loop containing the b quark. This leads to,

$$\tau_1(\tilde{\gamma} \rightarrow \gamma\nu + \gamma\overline{\nu}) \sim 10^{-9}\text{sec}(m_{\tilde{q}_3}/100 \text{ GeV})^4(1 \text{ GeV}/m_{\tilde{\gamma}})^3 \text{ x } (1/C_3)^2 \ . \tag{45}$$

It is clear that in order to have the photino decay within a detector, we must have $m_{\tilde{q}_3}^2/C_3 \lesssim (180 \text{ GeV})^2$ for a 1 GeV photino.

In the case where the dominant contribution to photino decay is from sneutrino VEVs, the diagrams of Figure 5 contribute. We evaluate the contribution from Figure 5a as representative,

$$\Gamma_2(\tilde{\gamma} \rightarrow \gamma\nu + \gamma\overline{\nu}) \sim (\alpha^4 \tilde{v}_a{}^2 m_{\tilde{\gamma}}^3)/(64\pi \sin^4\theta_W)[1/(m_{\tilde{l}_a}^2 - M_W^2)^2] \text{ x } [\ln(m_{\tilde{l}_a}^2/M_W^2)]^2 \ . \tag{46}$$

For reasonable choices of the parameters this gives

$$\tau_2(\tilde{\gamma} \rightarrow \gamma\nu + \gamma\overline{\nu}) \sim 10^{-9}\text{sec}(m_{\tilde{l}_a}/100 \text{ GeV})^4(10 \text{ GeV}/\tilde{v}_a)^2 \text{ x } (1 \text{ GeV}/m_{\tilde{\gamma}})^3. \tag{47}$$

In theories with explicit lepton number violation, it may also be possible to have the decay $\tilde{\gamma} \rightarrow l_a\overline{l}_a\nu$ or $\tilde{\gamma} \rightarrow q_i\overline{q}_i\nu$. The diagram of Figure 6 gives the decay width,

$$\Gamma_3(\tilde{\gamma} \rightarrow l_a\overline{l}_a\nu + l_a\overline{l}_a\overline{\nu}) \sim \frac{\alpha D_a^2}{128\pi^2}\frac{m_{\tilde{\gamma}}^5}{m_{\tilde{l}_a}^4} \ . \tag{48}$$

(The rate for $\tilde{\gamma} \to q_i\overline{q_i}\nu$ is obtained by multiplying Eq. (48) by $3e_q^2$ and replacing $D_a \to C_a$ and $m_{\tilde{l}_a} \to m_{\tilde{q}_a}$). This gives a lifetime,

$$\tau_3(\tilde{\gamma} \to l_a\overline{l_a}\nu + l_a\overline{l_a}\overline{\nu}) \sim 10^{-11}\text{sec}(m_{\tilde{l}_a}/100\text{ GeV})^4(1\text{ GeV}/m_{\tilde{\gamma}})^5(1/D_a)^2 \; . \tag{49}$$

(Note that in models with non-zero sneutrino VEVs the mixing in the lepton sector will introduce the off diagonal decays $\tilde{\gamma} \to l_a\bar{l}_b\nu$.) Thus depending upon the parameters of the model, photino decays may lead to observable tracks in the detector. Certainly, for a large range of reasonable parameters, the photino will decay within the detector.

4.3 New Signals

Finally, we consider the effects of the new decay patterns on the signals expected from SUSY particle production. As examples, we consider two processes: $p\overline{p} \to \tilde{\gamma}\tilde{g}$ and $p\overline{p} \to \tilde{g}\tilde{g}$. If the photino is stable (and lighter than the gluino), then we expect $\tilde{g} \to q\overline{q}\tilde{\gamma}$. Then the signal for $p\overline{p} \to \tilde{\gamma}\tilde{g}$ is ≤ 2 jets plus missing p_T and for $p\overline{p} \to \tilde{g}\tilde{g}$ it is ≤ 4 jets plus missing p_T. If the $\tilde{\gamma}$ decays to $\gamma\nu$ then the signal for $\tilde{\gamma}\tilde{g}$ production will still be ≤ 2 jets plus missing p_T, but in addition there will be a photon and the $\tilde{\gamma}$ decay will degrade the missing p_T signal. If the photino decays to $q\overline{q}\nu$, then the signal for $\tilde{\gamma}\tilde{g}$ production will be ≤ 6 jets plus a degraded missing p_T signal . For $\tilde{g}\tilde{g}$ production, the signal will be ≤ 4 jets plus two photons if $\tilde{\gamma} \to \gamma\nu$ and ≤ 8 jets if $\tilde{\gamma} \to q\overline{q}\nu$. In all cases, the decay of the photino leads to a degraded missing p_T signal which yields significantly smaller cross sections since fewer events will pass a given missing p_T cut.

To analyze these decay modes we use a Monte Carlo program

and approximate the UA1 cuts [14]. We require that the missing energy, E_T^m, satisfy,

$$\begin{aligned} &E_T^m \geq 4\sigma \qquad \text{where } \sigma = .7\sqrt{E_T} \\ \text{and} \quad & \\ &E_T^m \geq 32\text{ GeV} \; . \end{aligned} \tag{50}$$

E_T is the scalar sum of the transverse energy. E_T cannot be calculated within the parton model since it contains energy from the spectator quarks as well as the interacting quarks. We approximate E_T by including in it the energy of all the final state interacting quarks whether or not they are included in a jet [15]. We also include in E_T the photon energy in the case $\tilde{\gamma} \to \gamma\nu$.

In addition E_T^m must not point to within $\pm 20^{o}$'s of the vertical because of reduced calorimetry in this region. We use the UA1 jet algorithm and define a jet by adding up all the energy within a cone described by $\Delta\phi^2 + \Delta\eta^2 \leq 1$. Also, the most energetic jet must have $E_T^j \geq 25$ GeV and all other jets must have $E_T^j \geq 12$ GeV. Finally, one jet events are rejected if $\cos\Delta\phi \geq -.8$. (This is to reject the tail of the two jet QCD background). We interpret all final state quarks as hadronic jets if they pass the cuts described above.

In Figures 7a and 7b, we show the E_T^m spectrum at $\sqrt{s} = 540$ GeV for $\tilde{\gamma}\tilde{g}$ production in $p\overline{p}$ collisions assuming stable $\tilde{\gamma}$, $\tilde{\gamma} \to \gamma\nu$, and $\tilde{\gamma} \to q\overline{q}\nu$ and for $m_{\tilde{g}} = 40$ GeV and 60 GeV, respectively. In both cases we have taken $m_{\tilde{q}} = 100$ GeV and $m_{\tilde{\gamma}} = 1$ GeV [16]. The E_T^m spectra include all of the events which pass the cuts which have at least one jet. In Figures 8a and 8b we show the transverse mass spectrum under the same set of assumptions. The most striking feature of these plots is the degrading of the missing p_T signal if the photino is allowed to decay. Only about 1/100 as many events pass the cuts if $\tilde{\gamma} \to q\bar{q}\nu$ as for a stable photino.

In Figures 9a and 9b, we plot the E_T^m spectrum for $\tilde{g}\tilde{g}$ production assuming $\tilde{g} \to q\bar{q}\tilde{\gamma}$ and for stable $\tilde{\gamma}$, $\tilde{\gamma} \to \gamma\nu$, and $\tilde{\gamma} \to q\bar{q}\nu$ and in Figures 10a and 10b we plot the transverse mass. Again we note the drastic degrading of the missing p_T signal. From Figures 7 - 10, we conclude that if the photino decays, the search for supersymmetry will be extremely difficult. The generic missing p_T signal is degraded and could easily become lost in the heavy quark background.

The different photino decay modes change the ratio of monojets to dijets. In Figure 11 we show the one and two jet cross sections for gluino pair production as a function of the gluino mass (and for fixed squark mass) for each of the assumed photino decay patterns. The largest jet cross sections result when the photino is stable, with the two jet cross section becoming larger than the one jet cross section for a gluino mass between 40 and 50 GeV. The jet cross sections are approximately an order of magnitude smaller when the photino decays to $\gamma\nu$. This is because we have included the photon energy in our definition of E_T which means that fewer of the events can pass the E_T^m cut. The jet cross sections are considerably smaller when $\tilde{\gamma} \to q\bar{q}\nu$ with the two jet cross section always dominating over the one jet cross section. In this case the three jet cross section becomes dominant for gluino masses greater than about 60 GeV.

5 Conclusion

Low energy supersymmetric models can violate lepton num-

ber either explicitely or spontaneously through the VEVs of scalar neutrinos. Although both possibilities are unattractive, explicit lepton number violating interactions are allowed by the SU(3) x SU(2) x U(1) gauge symmetries and must be forbidden by imposing discrete symmetries . Similarly, the scalar potential will naturally allow the sneutrinos to obtain VEVs if the soft lepton number violating terms of Eq. (10) are allowed. The experimental limits on explicit lepton number violating interactions are quite weak, allowing coefficients on the order of 10^{-3} for these operators. Models with explicit or spontaneous lepton number violation are thus experimentally viable.

In supersymmetric models with $\tilde{R}$ parity violation the phenomenology will be quite different from the usual SUSY theories. Single production of SUSY particles, while having small cross sections in most models, will lead to spectacular new signals. These cross sections, unfortunately, will probably only be measurable for extremely light SUSY particles. The most striking new signature ,however, will be the decay of the photino which leads to degraded missing p_T signatures. This will considerably complicate the search for supersymmetry!

ACKNOWLEDGEMENTS

This work was supported by the Director, Office of Energy Research, Office of High Energy and Nuclear Physics, Division of High Energy Physics of the U.S. Department of Energy under Contract DE-AC03- 76SF00098.

REFERENCES

[1] S. Dawson, E. Eichten, and C. Quigg, Phys. Rev. D31 (1985) 1581; H. Haber and G. Kane, Phys. Rep. 117 (1985) 75.

[2] R. M. Barnett, H. Haber, and G. Kane, LBL-18990, January 1985.

[3] J. Ellis and H. Kowalski, Nucl. Phys. B246 (1984) 198; A. Allen, E. Glover, and A. Martin, Phys. Lett. 146B (1984) 247; V. Barger, K. Hagiwara, W. Keung, and J. Woodside, Phys. Rev. D31 (1985) 528.

[4] R symmetry breaking in supersymmetric theories has been considered by G. Farrar and S. Weinberg, Phys. Rev. D27 (1983) 2734.

[5] L. Hall and H. Suzuki, Nucl. Phys. B231 (1984) 419.

[6] I. Lee, Nucl. Phys. B246 (1984) 120.

[7] J. Ellis, G. Gelmini, C. Jarlskog, G. Ross, and J. Valle, Phys. Lett. 150B (1985) 142.

[8] C. Aulakh and R. Mohapatra, Phys. Lett 119B (1982) 136.

[9] G. Ross and J. Valle, Phys. Lett. 151B (1985) 375.

[10] L. Alvarez-Gaume, J. Polchinski, and M. Wise, Nucl. Phys. B221 (1983) 495; L. Hall, J. Lykken, and S. Weinberg, Phys. Rev. D27 (1983) 2359.

[11] The authors of Ref. [5] have considered explicit lepton number violating interactions which are not diagonal in generation space. This additional complication does not change any of the conclusions in Section 4.

[12] H. Georgi, S. Glashow, S. Nussinov, Nucl. Phys. B193 (1981) 297; M. Fukugita, S. Watamura, M. Yoshimura, Phys. Rev. Lett. 48 (1982) 1522.

[13] C. Matteuzzi et al., SLAC-PUB-3560, January 1985.

[14] G. Arnison et al., Phys. Lett. 139B (1984) 115; Phys. Lett. 136B (1984) 294.

[15] In order to properly simulate the UA1 $\not{E}_T^m$ cut, it is necessary to add about 40 or 50 GeV to $\not{E}_T$ to mock up the distribution of minimum bias events. However, our cut on $\not{E}_T^m \geq 32$ GeV greatly reduces the sensitivity to the definition of $\not{E}_T$. I thank H. Haber for a discussion of this point.

[16] We have assumed that the decay $\tilde{\gamma} \rightarrow \gamma\nu$ occurs through the explicit lepton number violating terms of Eq. (10) and have taken $C_3 = D_3 = 1$. Our results are not sensitive to this assumption.

FIGURE CAPTIONS

Figure 1 Solutions to the minimization of the scalar potential in a model with one generation. Figure 1 shows $\tan\gamma = \tilde{v}_1/v_2$ as a function of $\tilde{m}/\tilde{M}$ and $\mu_4/\tilde{M}$. The solid, dashed, dot-dashed, and dotted lines have $\mu_4/\tilde{M}$ =7 x 10^{-3}, $10^{-2}, 10^{-1}$ and .3, respectively.

Figure 2 Feynman diagram which gives the neutrinos mass.

Figure 3 Cross sections for $p\bar{p} \rightarrow \tau\tilde{g}$ at $\sqrt{s} = 540$ GeV (solid line) and 2 TeV (dashed line). We have assumed $\tilde{v}_\tau = 20$ GeV and $m_{\tilde{g}}$ =3 GeV.

Figure 4 Feynman diagrams for the decay $\tilde{\gamma} \rightarrow \gamma\nu$ which are proportional to C_a^2 .

Figure 5 Feynman diagrams for the decay $\tilde{\gamma} \rightarrow \gamma\nu$ which depend on the sneutrino VEVs.

Figure 6 Feynman diagram for the decay $\tilde{\gamma} \rightarrow q\bar{q}\nu$.

Figure 7 Missing p_T spectra for the reaction $p\bar{p} \rightarrow \tilde{\gamma}\tilde{g}$ at $\sqrt{s} = 540$ GeV. Fig. 7a has $m_{\tilde{g}} = 40$ GeV and Fig. 7b has $m_{\tilde{g}} = 60$ GeV. Both figures have $m_{\tilde{\gamma}}$ = 1 GeV and $m_{\tilde{q}} = 100$ GeV. The dashed line assumes a stable photino, the solid line $\tilde{\gamma} \rightarrow \gamma\nu$, and the dotted line $\tilde{\gamma} \rightarrow q\bar{q}\nu$.

Figure 8 Transverse mass spectra for one jet events in the reaction $p\bar{p} \rightarrow \tilde{\gamma}\tilde{g}$ at $\sqrt{s} = 540$ GeV. Fig. 8a has $m_{\tilde{g}} = 40$ GeV and Fig. 8b has $m_{\tilde{g}} = 60$ GeV. Both figures have $m_{\tilde{\gamma}} = 1$ GeV and $m_{\tilde{q}} = 100$ GeV. The dashed line assumes a stable photino, the solid line $\tilde{\gamma} \rightarrow \gamma\nu$, and the dotted line $\tilde{\gamma} \rightarrow q\bar{q}\nu$.

Figure 9 Missing p_T spectra for the reaction $p\bar{p} \to \tilde{g}\tilde{g}$ at $\sqrt{s}$ = 540 GeV. Fig. 9a has $m_{\tilde{g}}$ = 40 GeV and Fig. 9b has $m_{\tilde{g}}$ = 60 GeV. Both figures have $m_{\tilde{\gamma}}$ = 1 GeV and $m_{\tilde{q}}$ = 100 GeV. The dashed line assumes a stable photino, the solid line $\tilde{\gamma} \to \gamma\nu$, and the dotted line $\tilde{\gamma} \to q\bar{q}\nu$.

Figure 10 Transverse mass spectra for one jet events in the reaction $p\bar{p} \to \tilde{g}\tilde{g}$ at $\sqrt{s}$ = 540 GeV. Fig. 10a has $m_{\tilde{g}}$ = 40 GeV and Fig. 10b has $m_{\tilde{g}}$ = 60 GeV. Both figures have $m_{\tilde{\gamma}}$ = 1 GeV and $m_{\tilde{q}}$ = 100 GeV. The dashed line assumes a stable photino, the solid line $\tilde{\gamma} \to \gamma\nu$, and the dotted line $\tilde{\gamma} \to q\bar{q}\nu$.

Figure 11 Jet cross sections for the reaction $p\bar{p} \to \tilde{g}\tilde{g}$ at $\sqrt{s}$ = 540 GeV. The solid lines are the one jet cross sections and the dashed lines are the two jet cross sections. The three sets of curves represent a stable $\tilde{\gamma}$, $\tilde{\gamma} \to \gamma\nu$, and $\tilde{\gamma} \to q\bar{q}\nu$.

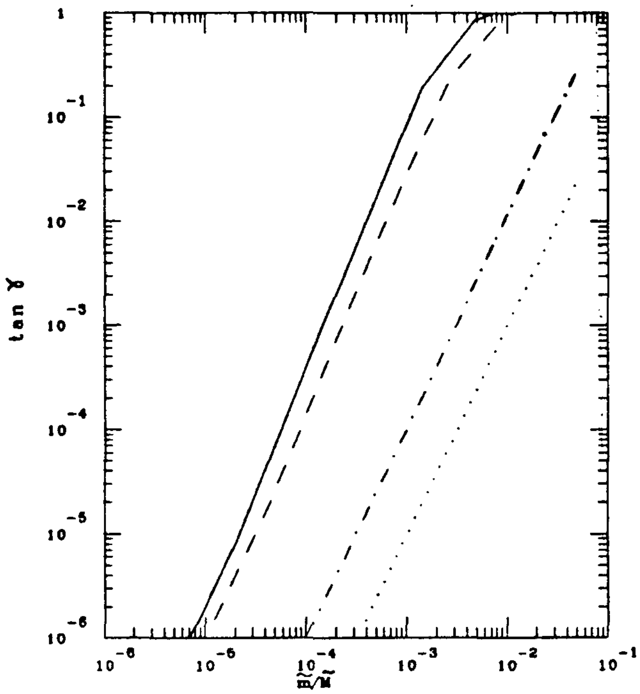

Figure 1

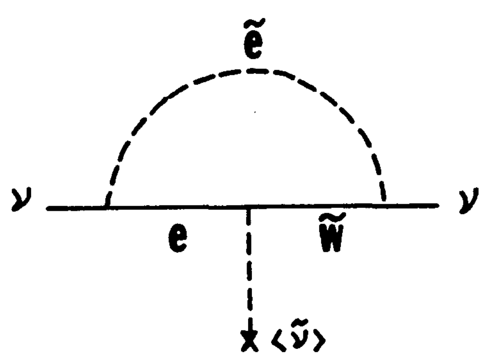

Figure 2

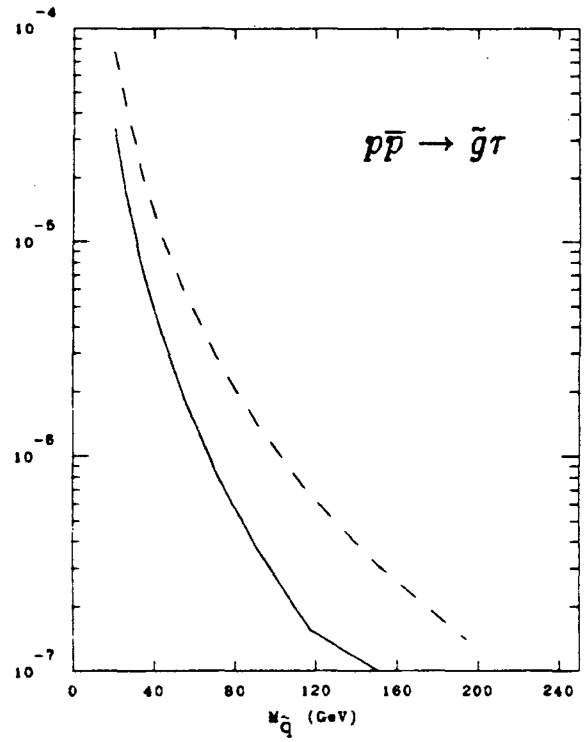

Figure 3

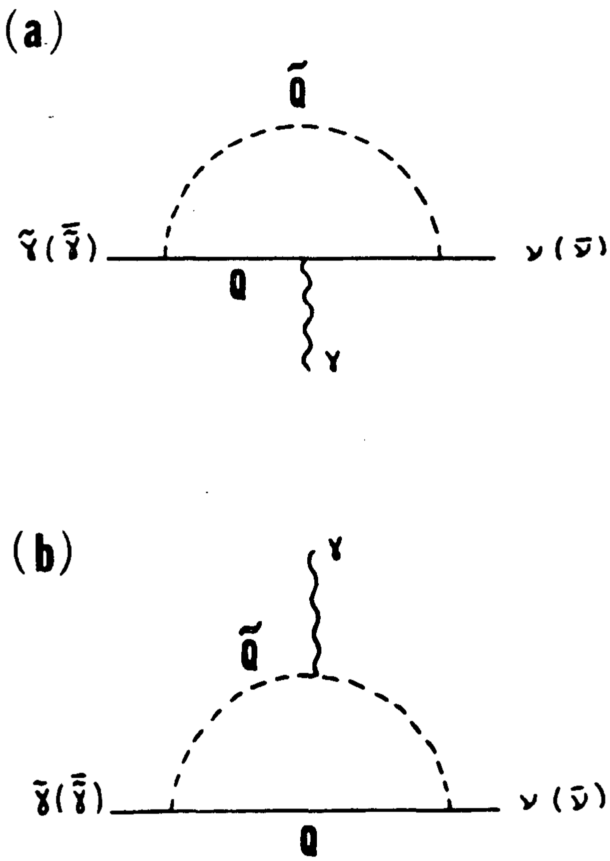

Figure 4

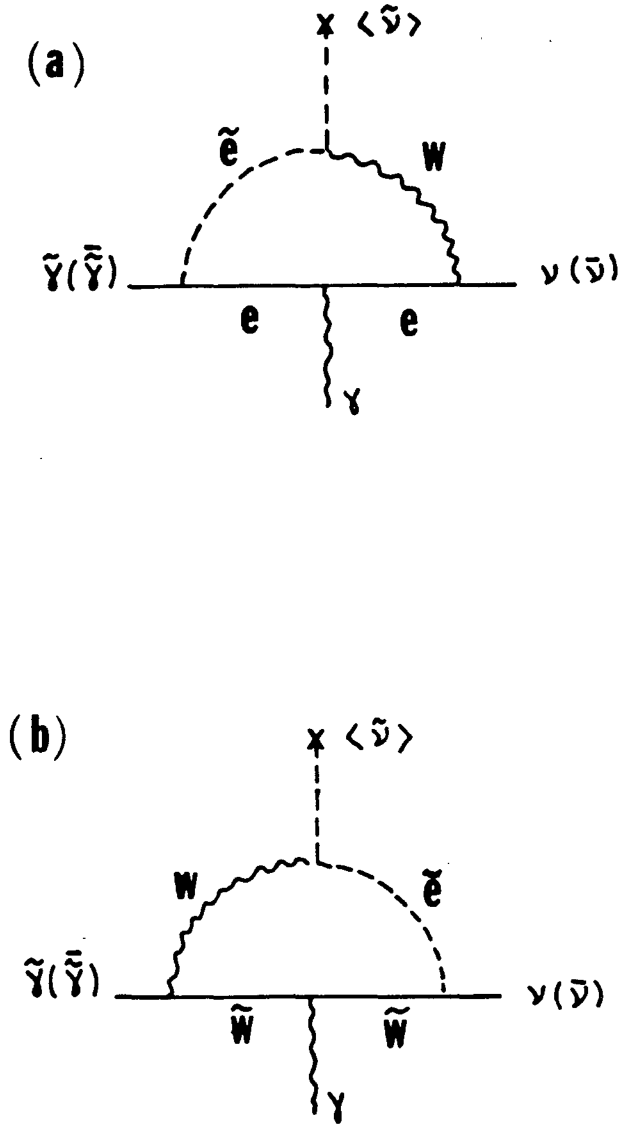

Figure 5

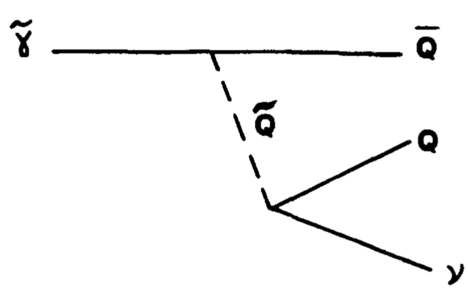

Figure 6

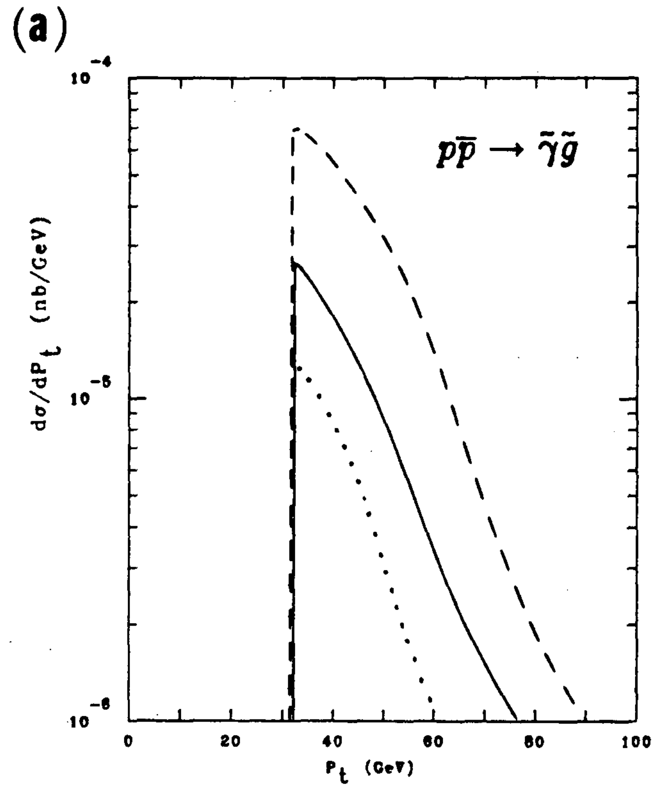

Figure 7a

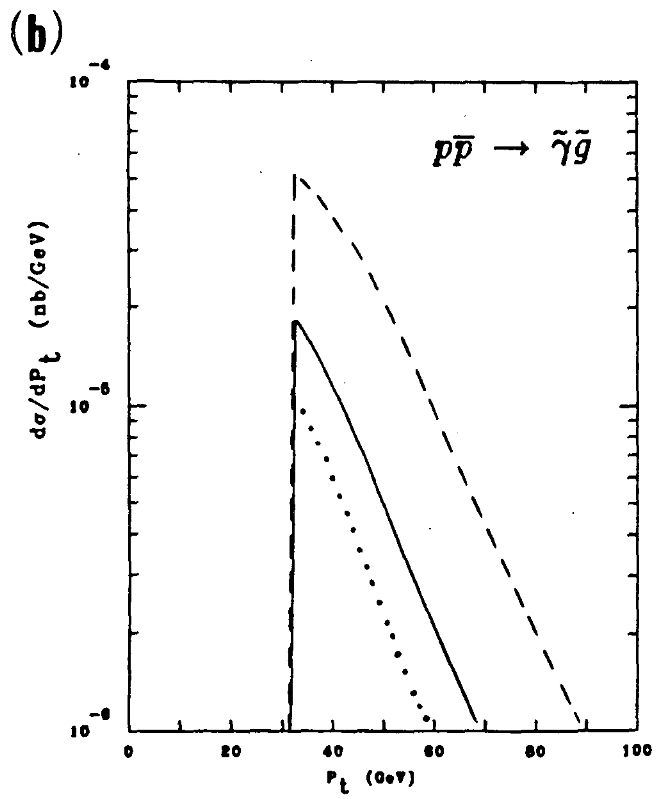

Figure 7b

(a)

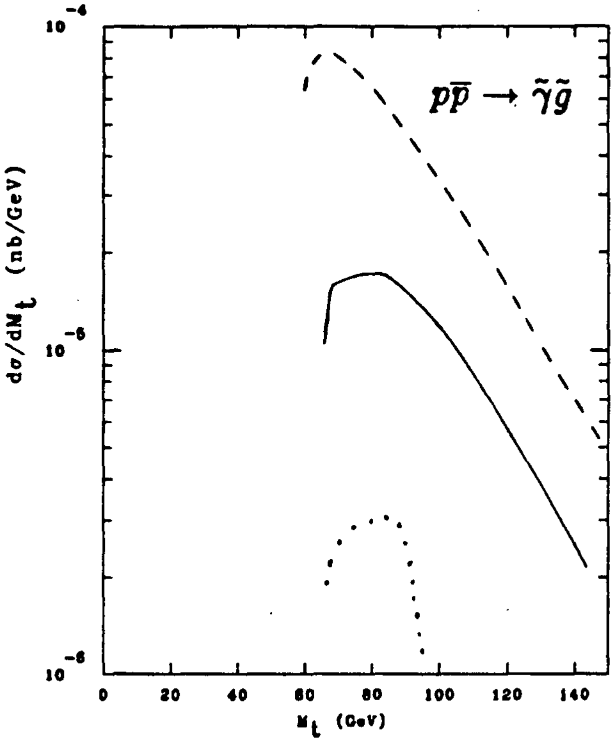

Figure 8a

(b)

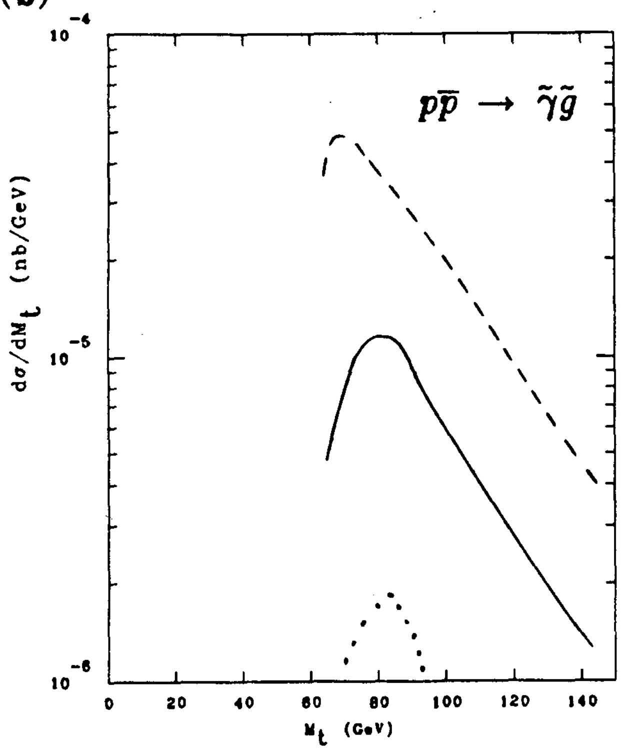

Figure 8b

(a)

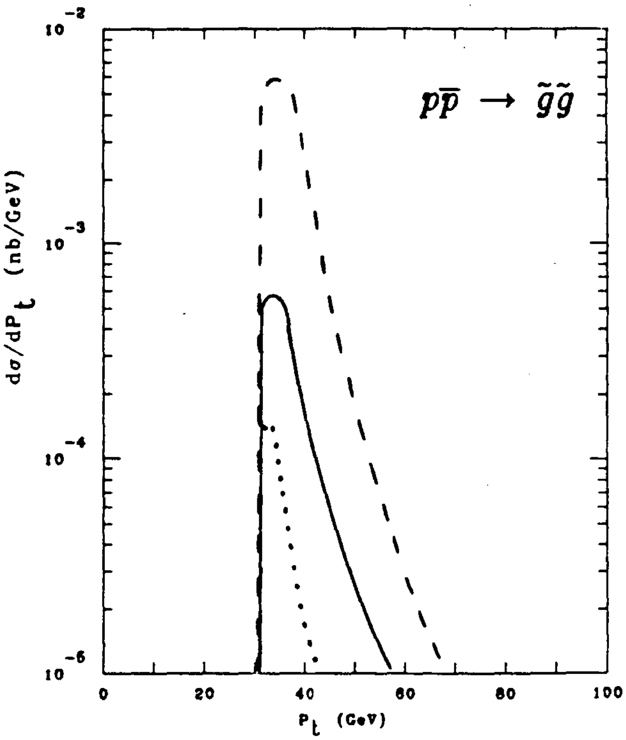

Figure 9a

(b)

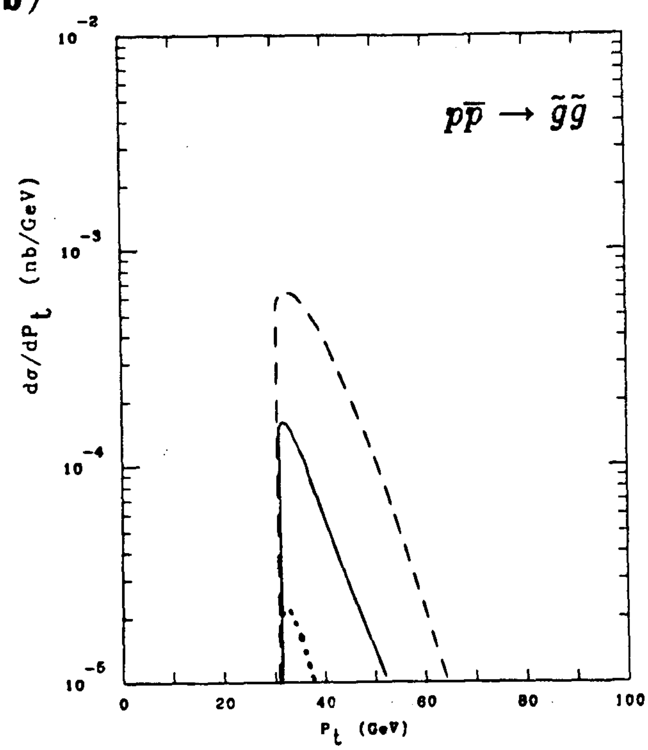

Figure 9b

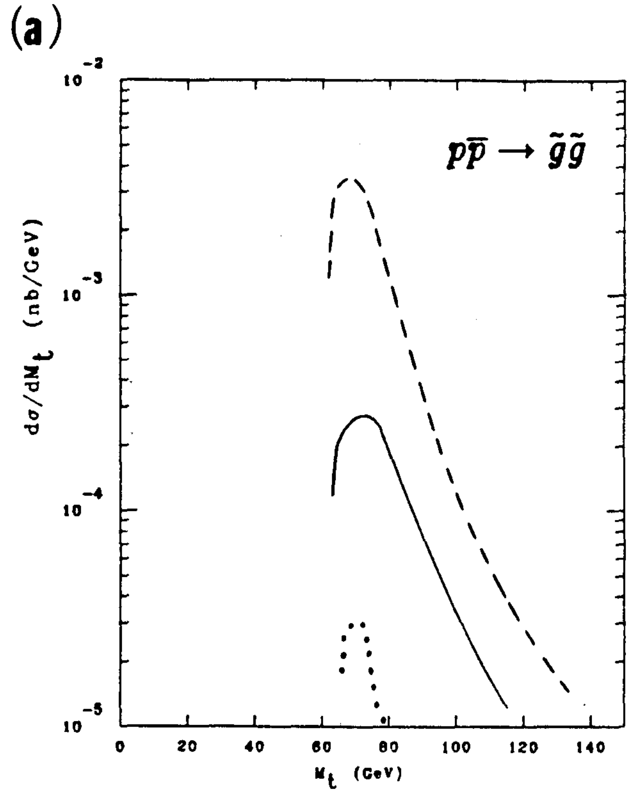

Figure 10a

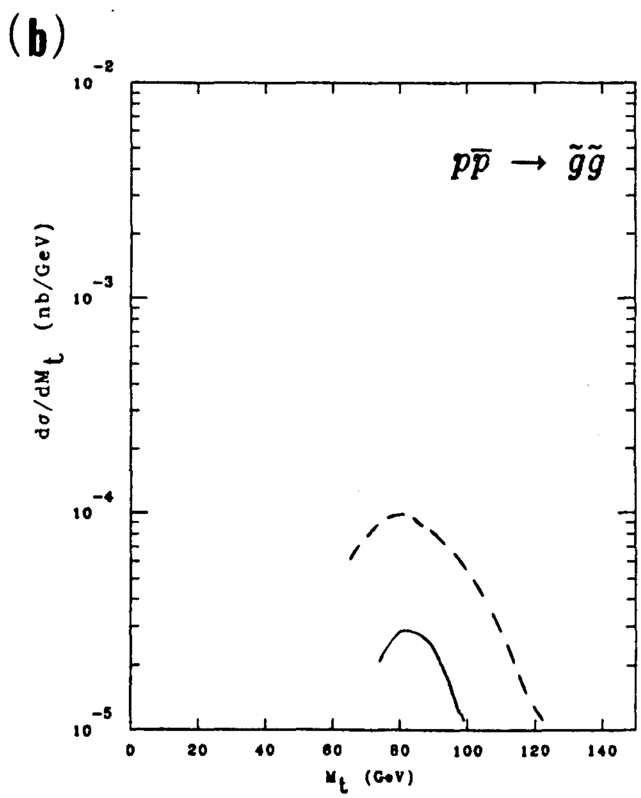

Figure 10b

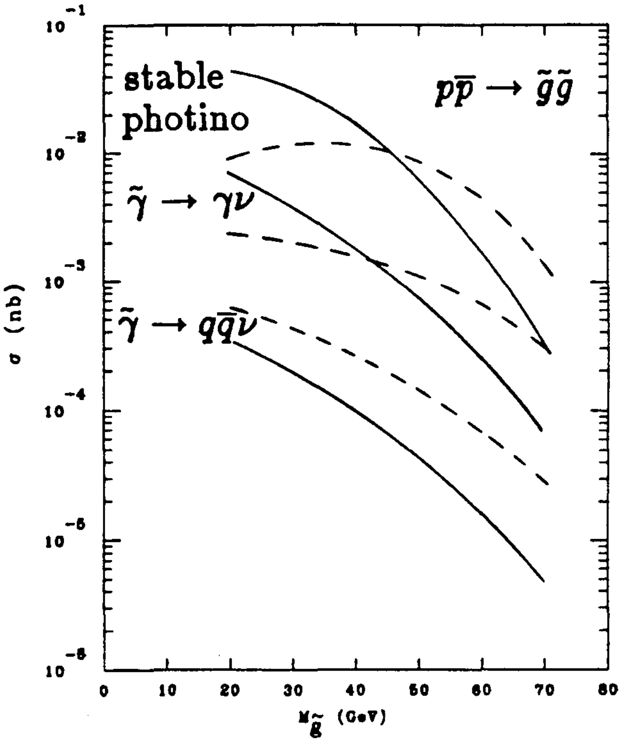

stable photino
$p\bar{p} \to \tilde{g}\tilde{g}$
$\tilde{\gamma} \to \gamma\nu$
$\tilde{\gamma} \to q\bar{q}\nu$
σ (nb)
$M_{\tilde{g}}$ (GeV)

Figure 11